IASS 2018 BOSTON, JULY 16-20
CREATIVITY IN STRUCTURAL DESIGN

Proceedings of the IASS Symposium 2018
Creativity in Structural Design
July 16-20, 2018, MIT, Boston, USA
Caitlin Mueller, Sigrid Adriaenssens (eds.)

Developing Algebraic Constraints for Reciprocal Polyhedral Diagrams of 3D Graphic Statics

Masoud AKBARZADEH*[,a], Márton HABLICSEK[a], Yi GUO[a]

[*,a] Polyhedral Structures Laboratory, School of Design, University of Pennsylvania, Philadelphia, USA
Pennovation Center, 3401 Grays Ferry Ave. Philadelphia, PA, 19146
masouda@upenn.edu

Abstract

3D graphic statics using reciprocal polyhedral diagrams (3DGS) is one of the recent developments in the field of geometry-based structural form finding and is a powerful method in generating spatial structural forms and their force diagram in three dimensions. However, constructing reciprocal polyhedral diagrams in 3D is quite challenging and the research lacks a rigorous mathematical definition formulating the geometrical and reciprocal relationship between the form and force diagrams in 3DGS. Having been used for the past 150 years, 2D graphic statics has recently been formulated algebraically that allows better topological understanding the relationship between the form and the force diagrams in 2D. Such algebraic formulation is crucial in developing interactive tools enabling designers and practitioner to exploit the potentials of working with the form and force diagrams by computationally drawing the reciprocal diagrams for each design iteration which was otherwise quite tedious and cumbersome. This paper provides initial formulation of the reciprocal relationships between polyhedral form and the force diagrams in 3DGS and lays a foundation for further research in algebraic implementation of 3DGS.

Keywords: Algebraic methods, 3D graphic statics, reciprocal constructions, constraint equations

1. Introduction

In the past decade, geometry-based structural design methods, commonly known as Graphic Statics, have received much attention from researchers in the field of structural design and architecture for their unprecedented control in design, form finding and optimization of unique structural solutions (Van Mele et al. [1], Beghini et al. [2], Akbarzadeh [3], Lee et al. [4], and McRobie [5]). However, the procedural graphic statics as it was practiced in the late nineteenth century is quite cumbersome and time-consuming (Maxwell [6], Cremona [7], and Wolfe [8]). The geometry-based techniques in combination with computational methods result in innovative design tools allowing the further exploration of the realm of sophisticated, yet efficient structural equilibrium (Block [9]). Rhino Vault is an excellent example that combines 2D reciprocal diagrams with the force density methods and allows for the design of free-form shell structures (Rippmann et al. [10], Sheck [11]).

The algebraic implementation of the conventional/2D graphic statics is another valuable example that allows the interactive manipulation of both form and force diagrams, and therefore, indeed exploits the pedagogical potential of graphical methods in the age of computational power (Van Mele and Block [12], Alic and Åkesson [13]). This formulation provides a rigorous understanding and control of various characteristics of the systems such as geometric degrees of freedom and the degrees of indeterminacies of complex structural forms and their reciprocal force diagrams. As a result, a user can control the magnitude the forces in specific edges of the form diagram (members of the structure) as well as some essential geometric properties such as the length and the location of the supports without disturbing the internal and external equilibrium [12, 13].

1.1. Problem Statement and Objectives

3D Graphical statics is a recent development of the geometric principles of equilibrium in three dimensions based on a historical proposition by Rankine [14] and Maxwell [6] in 1864 [3, 4, 5]. In 3DGS, the form and the force diagrams are reciprocal polyhedral diagrams that are topologically dual and geometrically perpendicular; the equilibrium of each node of a polyhedral frame with its applied/internal forces is represented by a closed force polyhedron whose faces are perpendicular to the forces of the node. The area of each face represents the magnitude of the corresponding force to keep the node in equilibrium.

The geometric construction of these reciprocal diagrams is the primary step in using 3DGS methods. Currently, there are multiple geometric approaches for the construction of these reciprocal polyhedrons. Akbarzadeh et al. provided an iterative approach in constructing the reciprocal form for a given system of polyhedral cells (Akbarzadeh et al. [15]). Although the iterative method is a robust way of constructing these reciprocal diagrams, the precise controlling the edge lengths are quite cumbersome: any manipulation introduced by the user in the geometry of the form breaks the equilibrium states and requires a new iterative process. In another approach, McRobie et al. suggest the projection of the polyhedral system to the fourth dimension and bring back to the third by using paraboloid of revolution [5]. Although this fundamental approach is quite robust, it might be relatively counter-intuitive for the users with limited experience with geometric constructions in 3D space.

Therefore, there is a lack of a proper mathematical formulation for construction of reciprocal diagrams of 3D graphic statics. Note that the algebraic 3DGS provides us with a better understanding of the geometric degrees of freedom of the polyhedral systems, and therefore, allows for the interactive manipulation of these diagrams for design purposes. Thus, the primary objective of this paper is to provide an algebraic approach to formulate and to construct these reciprocal polyhedrons. Moreover, the method of this research can be applied to both form and force polyhedrons to build their reciprocal diagram.

2. Theoretical Framework

This paper introduces the algebraic formulation for the determinate reciprocal polyhedral diagrams. Providing a complete algebraic formulation for constructing reciprocal diagrams of 3DGS with full control over edge lengths and the magnitude of forces for indeterminate cases is beyond the scope of this paper.

2.1. Reciprocal Polyhedrons in 3DGS

The form and force diagrams in the context of 3DGS have certain topological features that needs further explanation before the explanation of their algebraic relationships.

2.1.1. Form polyhedrons

Usually, in the context of 3DGS, we describe the form diagram as a group of polyhedrons with both open and closed cells. The open cells that are usually on the exterior of the system represent the applied forces and the location of the supports [15].

2.1.2. Force polyhedrons

The force diagram, on the other hand, consists of closed polyhedral cells. There is one cell in the group of polyhedrons that represents the global equilibrium of the system, and the rest of the cells represent the nodal equilibria. If the global force cell is the external force polyhedron in the system, then the system can describe the equilibrium of compression/tension-only system of forces (depending on the properties of the form diagram). The global force polyhedron can also be any other cell in the group of cells. Note that the direction of the faces of the global force polyhedron defines the direction of the faces of the interior cells: for each interior cell if it is adjacent to the global, it will have the same face directions. If the internal cell is adjacent to another internal, it will have the opposite face direction.

Topological relationships

Form and force polyhedrons are topologically dual and geometrically reciprocal. I.e. the vertices v, edges e, faces f and cells c of one diagram corresponds to cells c^*, faces f^*, edges e^* and vertices v^* correspondingly. In this context, we call the input diagram the *primal* and its reciprocal the *dual*. Moreover, each edge e of the primal is perpendicular to a face of the dual.

2.1.3. Input geometry

Whether we start from the force diagram or the form diagram, in both scenarios, we have one diagram open and the other one closed.

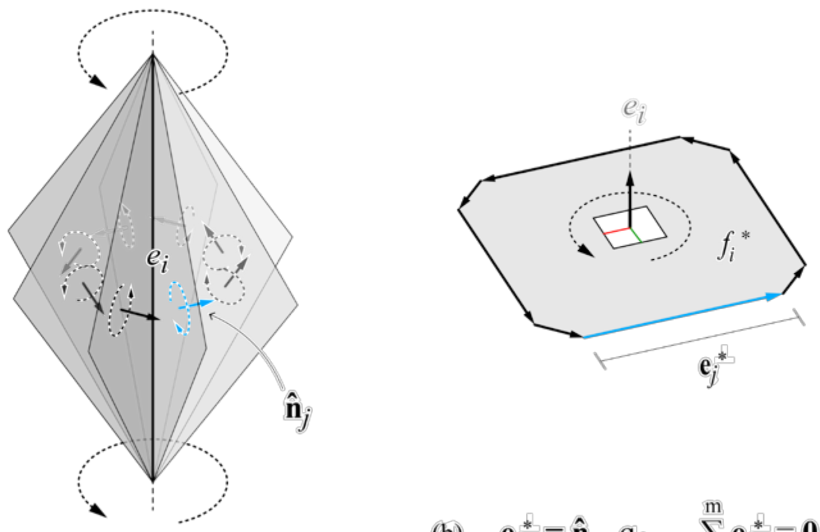

(a) (b) $\mathbf{e}_j^* = \hat{\mathbf{n}}_j \cdot q_j$, $\sum^{m} \mathbf{e}_j^* = \mathbf{0}$

Figure 1: Rounding each edge of the input with its attached faces (a) provides the direction of the edge vectors of the corresponding face (b) in the reciprocal diagram where sum of the edge vectors must be zero.

2.2. Developing the algebraic constraints

To develop the algebraic constraints, we revisit Maxwell's groundbreaking paper, "On reciprocal figures, frames and diagrams of forces" [6]. The excerpt of the paper denoting the idea is as follows:

"Round any edge of the first diagram draw a closed curve, embracing it and no other edge. However small the curve is, it will enter each of the cells which meet in the edge. Hence the reciprocal of this closed curve will be a plane polygon whose angles are the points reciprocal to these cells taken in order."

Simply put, consider an edge e_i of the primal diagram and all its attached faces f_1, f_2, ..., f_k (Fig. 1a). The edge e_i is reciprocal to a face f_i^* in the dual. By moving the thumb along the direction of the edge, the fingers curl around the edge going through its attached faces. Each normal $\hat{\mathbf{n}}_j$ of a face f_j is parallel to an edge vector $\mathbf{e}_j^*$ of the polygon f_i^* (Fig. 1b). Moreover, the direction of the edge vectors

$\mathbf{e}_j^*$ are consistent and the sum of the edge vectors around the polygon f_i^* should be zero. i.e. the sum of the unit normal $\hat{\mathbf{n}}_j$ times the length q_j of the edge vector $\mathbf{e}_j^*$ should be zero:

$$\pm\hat{\mathbf{n}}_1 q_1 \pm \hat{\mathbf{n}}_2 q_2 \pm \ldots \pm \hat{\mathbf{n}}_k q_k = 0 \quad (1)$$

Since the faces might have arbitrary directions, the $\hat{\mathbf{n}}_i$ of each face attached to the edge e_i:

$$\begin{cases} +\hat{\mathbf{n}}_i & \text{if matches the curl direction around } e_i \\ -\hat{\mathbf{n}}_i & \text{otherwise.} \end{cases}$$

2.3. Equilibrium matrix

Let us denote the $x-$, $y-$ and $z-$ coordinates of the vectors $\hat{\mathbf{n}}_i$ as n_{xi}, n_{y_i} and n_{zi} respectively. The vector equation 1 can be written as three linear equations and the equation 1 becomes:

$$\begin{cases} \pm n_{x1} q_1 \pm n_{x2} q_2 \pm \ldots \pm n_{xk} q_k = 0 \\ \pm n_{y_1} q_1 \pm n_{y_2} q_2 \pm \ldots \pm n_{y_k} q_k = 0 \\ \pm n_{z1} q_1 \pm n_{z2} q_2 \pm \ldots \pm n_{zk} q_k = 0 \end{cases} \quad (2)$$

These equations can be written in a linear equation system resulting in a $3e \times f$ matrix that we can call the equilibrium matrix **A**:

$$\mathbf{Aq} = \mathbf{0} \quad (3)$$

2.4. Reducing the number of equilibrium equations

In the previous sections, we showed how to obtain the constraint equations and the equilibrium matrix. However, the constraint equations may not be independent of each other. In the following sections, we propose two ways to decrease the number of constraint equations significantly.

2.4.1 The dependent equations around each edge

Section 2.2 showed that each interior edge of the primal polyhedral complex gives rise to three constraint equations. However, these equations are linearly dependent. Consider the very edge e_i of the Section 2.2 with its connected faces $f_{1\ldots k}$ and its reciprocal face f_i^* in the dual. Let us denote a vector parallel to the edge e_i by $\mathbf{e}_i$. The vector $\mathbf{e}_i$ is not only perpendicular to the face f_i^*, but it is also perpendicular to all the edge vectors $\mathbf{e}_j^*$ and all $\hat{\mathbf{n}}_{1\ldots k}$. Therefore, their dot products are zero:

$$\mathbf{e}_i \cdot \hat{\mathbf{n}}_1 = 0, \quad \mathbf{e}_i \cdot \hat{\mathbf{n}}_2 = 0, \quad \ldots, \quad \mathbf{e}_i \cdot \hat{\mathbf{n}}_k = 0.$$

As a consequence, we obtain that

$$\mathbf{e}_i \cdot (\pm\hat{\mathbf{n}}_1 q_1 \pm \hat{\mathbf{n}}_2 q_2 \pm \ldots \pm \hat{\mathbf{n}}_k q_k) = 0. \quad (4)$$

This implies that the three constraint equations in Equation system 2 are linearly dependent. In particular, the equilibrium matrix $\mathbf{A}$ can be reduced to a $[2e \times f]$ matrix.

2.4.2 The dependent equations of the adjacent faces

There is another way to reduce the number of constraint equations of the equilibrium matrix using topology. Each closed polyhedral cell c_i^* in the dual complex can be described by $f^* - 1$ faces where f^* denotes the number of faces of that cell. For a group of polyhedral cells $f^* - c^*$ faces are enough to completely describe the geometry where c^* denotes the number of cells. Since each face f_i^* and c_i^*

correspond to the edge e_i and vertex v_i of the primal then $e-v$ edges are enough to fully describe the geometry of the dual. Therefore, $2(e-v)$ equations are enough to complete the equilibrium matrix. Therefore, the equilibrium matrix **A** can be reduced to a $[2(e-v)\times f]$ matrix.

2.5. Solving equilibrium equations

The dimension of the solution vectors for the linear equation system 3 is $f-r$ where r is the rank of the equilibrium matrix **A**. For a determinate system, $f-r$ is 1, and therefore, we have a unique solution (up to scaling and translation). Since, the main concentration of this paper is to introduce the algebraic folmulation, solving the intederminate systems is beyond the scope of this paper.

2.6. The geometry of the dual

nce we obtained the edge lengths of the dual, we need to construct its polyhedral geometry by finding the coordinates of its vertices. The coordinates of the vertices can be found by having the topology and the direction of the edges of the dual to complete the geometry.

2.6.1. The topology of the dual and its edge directions

The connectivity of the edges e^* and vertices v^* that defines the topology of the dual can be easily found by establishing the connectivity of their reciprocal components, faces f and cells c, in the primal. Two adjacent cells c_i and c_j share a face f_k; that is, their dual vertices, v_i^* and v_j^*, are connected by an edge e_k^*. Note that the direction of the faces of a polyhedral cell in the primal is either towards inside or outside of the cell. If the direction of the face f_k in primal matches the direction of the same face in the cell c_i, then the tip of the edge e_k^* in the dual is at the vertex v_i^*; otherwise, at v_j^*.

2.6.2. The coorindates of the vertices

To find the coordinates of each vertex of the dual, we can establish a *tree* graph for the topology of the dual. The tree graph, in this case, is a graph with an arbitrary vertex, such as v_0^*, as the root that includes all paths to every other vertex of the dual starting from the root with no closed loop.To draw the geometry of the dual, each segment of the tree graph should acquire its length and direction. The length of each segment is identical to the length of each edge found in Section 2.5 and its direction follows the direction of the cell c_i reciprocal to the vertex v_i^* at the tip of the segment. Note that this direction might be different than the direction of the edge e_k^* as found in Section 2.6.1 By choosing an arbitrary coordinates for the root vertex v_0^*, the rest of the vertices can be found by translating the root using the segment vectors of each path.

2.7. The direction of the internal forces

We can specify the direction of forces in the members of the dual by matching the direction of the edge vector of the dual with the direction of a cell in the primal corresponding to the vertex at the tip of the vector. For instance, if the primal represents the force diagram, the type of force in the edge e_i^* of the form can be found as follows: if the edge vector e_i^*, a vector from v_j^* to v_k^*, is aligned with the direction of the normal $\hat{\mathbf{n}}_i$ of its corresponding face f_i in the cell c_k, the member is in compression; otherwise, it is in tension.

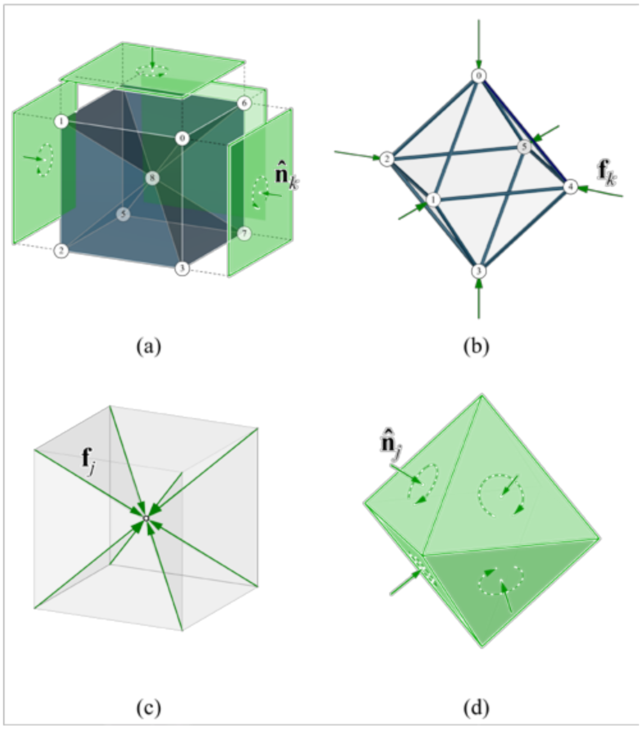

Figure 2: Input geometry as both form and force diagrams: (a) external polyhedron as the global force polyhedron; (b) the reciprocal compression-only form; (c) the input as the form and external polyhedron excluded to identify the applied forces, and (d) the reciprocal force diagram.

2.8. Example

In this section, we provide an explicit example demonstrating the theoretical explanations in the previous sections. Consider a polyhedral complex with its faces constructed as a cube with vertices at $(\pm 1, \pm 1, \pm 1)$ connected to a vertex at $(0,0,0)$ in its center. Therefore, the primal will include 8 external faces of the cube and 12 internal triangular faces with a vertex at the center sharing an edge with an external faces of the cube (Fig. 2[a]).

2.8.1 The equilbirum equations

For each interior face, we choose an arbitrary normal direction as:

$$\hat{\mathbf{n}}_1 = (-2,2,0),\quad \hat{\mathbf{n}}_2 = (0,2,2),\quad \hat{\mathbf{n}}_3 = (2,2,0),\quad \hat{\mathbf{n}}_4 = (0,-2,2),$$

$$\hat{\mathbf{n}}_5 = (2,0,-2),\quad \hat{\mathbf{n}}_6 = (-2,0,-2),\quad \hat{\mathbf{n}}_7 = (-2,0,2),\quad \hat{\mathbf{n}}_8 = (-2,0,-2),$$

$$\hat{\mathbf{n}}_9 = (2,2,0),\quad \hat{\mathbf{n}}_{10} = (0,2,-2),\quad \hat{\mathbf{n}}_{11} = (-2,2,0),\quad \hat{\mathbf{n}}_{12} = (0,2,2)$$

The equilibrium vector equations around the edges e_1, e_2, ..., e_8 are the following:

$$\begin{cases} q_1\hat{\mathbf{n}}_1 + q_4\hat{\mathbf{n}}_4 + q_5\hat{\mathbf{n}}_5 = 0 \\ q_1\hat{\mathbf{n}}_1 - q_2\hat{\mathbf{n}}_2 - q_6\hat{\mathbf{n}}_6 = 0 \\ q_2\hat{\mathbf{n}}_2 - q_3\hat{\mathbf{n}}_3 - q_7\hat{\mathbf{n}}_7 = 0 \\ q_3\hat{\mathbf{n}}_3 - q_4\hat{\mathbf{n}}_4 - q_8\hat{\mathbf{n}}_8 = 0 \\ q_5\hat{\mathbf{n}}_5 - q_9\hat{\mathbf{n}}_9 + q_{12}\hat{\mathbf{n}}_{12} = 0 \\ q_6\hat{\mathbf{n}}_6 - q_9\hat{\mathbf{n}}_9 - q_{10}\hat{\mathbf{n}}_{10} = 0 \\ q_7\hat{\mathbf{n}}_7 + q_{10}\hat{\mathbf{n}}_{10} - q_{11}\hat{\mathbf{n}}_{11} = 0 \\ q_8\hat{\mathbf{n}}_8 - q_{11}\hat{\mathbf{n}}_{11} + q_{12}\hat{\mathbf{n}}_{12} = 0 \end{cases}$$

These 8 equations can be written as 24 linear equations once we write the equations in terms of the $x-$, $y-$ and $z-$ coordinates. Explicitly, the part of the Equilibrium matrix A corresponding to the $x-$coordinates is the following:

$$\mathbf{A}_x = \begin{pmatrix} -2 & 0 & 0 & 0 & 2 & 0 & 0 & 0 & 0 & 0 & 0 & 0 \\ -2 & 0 & 0 & 0 & 0 & 2 & 0 & 0 & 0 & 0 & 0 & 0 \\ 0 & 0 & -2 & 0 & 0 & 0 & 2 & 0 & 0 & 0 & 0 & 0 \\ 0 & 0 & 2 & 0 & 0 & 0 & 0 & 2 & 0 & 0 & 0 & 0 \\ 0 & 0 & 0 & 0 & 2 & 0 & 0 & 0 & 2 & 0 & 0 & 0 \\ 0 & 0 & 0 & 0 & 0 & -2 & 0 & 0 & 2 & 0 & 0 & 0 \\ 0 & 0 & 0 & 0 & 0 & 0 & -2 & 0 & 0 & 0 & 2 & 0 \\ 0 & 0 & 0 & 0 & 0 & 0 & 0 & -2 & 0 & 0 & 2 & 0 \end{pmatrix}$$

We can see that the vector $\mathbf{q} = \mathbf{1}$ satisfies $\mathbf{A_x q} = \mathbf{0}$. Similarly, one can show that it actually satisfies the equation system 3 as well. Indeed the edge lengths of the dual complex are all equal.

2.8.2 Constructing the geometry of the dual

The topology of the dual can be found by the connectivity of the cells in the primal as explained in Section 2.6.1. There are six interior cells $c_{0\ldots5}$ in the primal that are reciprocal to six vertices in the dual $v^*_{0\ldots5}$. There are 12 faces $f_{0\ldots11}$ that are shared between every two cells that gives the edges $e^*_{0\ldots11}$ of the dual. We can find the tree graph for the topology of the dual as it was explained in Section 2.6.2. Starting the root of the tree at v^*_0, all the paths $p_{0\ldots4}$ from the root to complete the tree graph are the followings:

$$\begin{cases} p_0 = (0,1) \\ p_1 = (0,2) \\ p_2 = (0,1,3) \\ p_3 = (0,4) \\ p_4 = (0,5) \end{cases}$$

Note that in this case, path p_2 has two segments from v^*_0 to v^*_1 and from v^*_1 to v^*_3. By choosing the coordinates of the root vertex v^*_0, the rest of the vertices can be found using the edge lengths $q_{i\ldots k}$ from the previous section and the direction of the cells corresponding to the tip of each segment in the path.

2.8.3 The input as form diagram

The same procedure can be used to construct the force diagram for a given form polyhedron. I.e. the primal can be considered as the form diagram (Fig. 2b). In this case, one polyhedral cell should be considered as the applied forces (in this case the external), and all the edges connected to the vertices of the chosen polyhedron will be the applied forces to the system. Writing the equilibrium equations around all the edges of the system except the edges of the external polyhedron gives an equilibrium matrix resulting in the force distribution of the given form (Fig. 2c).

3. Conclusions and future work

This paper provided the algebraic formulation for construction of polyhedral reciprocal diagrams of 3DGS. The same formulation can be used to analyze and construct indeterminate polyhedral systems, but solving the equilibrium equations to control the area of faces and the use of geometric degrees of indeterminacies in manipulating the polyhedral systems will be addressed in the next stages of this research.

References

[1] T. Van Mele, L. Lachauer, M. Rippmann, and P. Block. "Geometry-based understanding of structures," *Journal of the International Association for Shell and Spatial Structures*, 2012, vol. 53, no. 174, pp. 285–295.

[2] L. L. Beghini, J. Carrion, A. Beghini, A. Mazurek, and W. F. Baker. "Structural optimization using graphic statics," *Structural and Multidisciplinary Optimization*, vol. 49, no. 3, pp. 351–366, 2014.

[3] M. Akbarzadeh, 3D *Graphical Statics Using Reciprocal Polyhedral Diagrams*, ETH Zurich, Stefano Franscini Platz 5, Zurich, CH, 8093, 2016.

[4] J. Lee, T. V. Mele, and P. Block, "Area-controlled construction of global force polyhedra," *IASS 2017: Interfaces - Architecture. Engineering. Science,* Hamburg, 2017.

[5] A. McRobie, "Maxwell and Rankine reciprocal diagrams via Minkowski sums for two-dimensional and three-dimensional trusses under load," *International Journal of Space Structures,* vol. 31, no. 2–4, pp. 203–216, June. 2016.

[6] Maxwell J.C., "On Reciprocal Figures, Frames, and Diagrams of Forces," *Transactions of the Royal Society of Edinburgh*, 1870; **7**; 160–208.

[7] L. Cremona, *Graphical Statics: Two treatises on the graphical calculus and reciprocal figures in graphical statics*, Translated by Thomas Hudson Beare, Clarendon Press, Oxford, 1890.

[8] W. S. Wolfe, *Graphical Analysis: A Text Book on Graphic Statics*. McGraw-Hill book Company, Incorporated, 1921.

[9] P. Block, *Thrust network analysis: exploring three-dimensional equilibrium*, PhD thesis, MIT, Cambridge, MA, USA, 2009.

[10] M. Rippmann, L. Lachauer and P. Block, "Interactive vault design", *International Journal of Space Structures*, vol. 27, no. 4, pp. 219-230

[11] H. J. Schek, "The force density method for form finding and computation of general networks," *Computer Methods in Applied Mechanics and Engineering*, 1974, vol. 3, no. 1, pp. 115–134.

[12] T. Van Mele and P. Block, "Algebraic Graph Statics," *Computer-Aided Design*, vol. 53, no. 37, pp. 104-116, 2014.

[13] V. Alic and D. Åkesson, "Bi-directional algebraic graphic statics," *Computer-Aided Design*, vol. 93, pp. 26-37, 2017.

[14] W.J.M. Rankine, "XVII. Principle of the equilibrium of polyhedral frames," *Philosophical Magazine* Series 4, vol. 27, no. 180, pp. 92–92, 1864.

[15] M. Akbarzadeh, T. Van Mele and P. Block, "Compression-only form finding through finite subdivision of the external force polygon," *Proceedings of the IASS-SLTE Symposium 2014*, Brasilia, Brazil, 2014.